Neurobiology of Disease

Working Memory Impairment in Calcineurin Knock-out Mice Is Associated with Alterations in Synaptic Vesicle Cycling and Disruption of High-Frequency Synaptic and Network Activity in Prefrontal Cortex

Jeffrey R. Cottrell,[1]* Jonathan M. Levenson,[1]* Sung Hyun Kim,[2] Helen E. Gibson,[1] Kristen A. Richardson,[1] Michael Sivula,[1] Bing Li,[1] Crystle J. Ashford,[1] Karen A. Heindl,[1] Ryan J. Babcock,[1] David M. Rose,[1] Chris M. Hempel,[1] Kjesten A. Wiig,[1] Pascal Laeng,[1] Margaret E. Levin,[1] Timothy A. Ryan,[2] and David J. Gerber[1]

[1]Galenea Corporation, Wakefield, Massachusetts 01880, and [2]Department of Biochemistry, Weill Cornell Medical College, New York, New York 10021

Working memory is an essential component of higher cognitive function, and its impairment is a core symptom of multiple CNS disorders, including schizophrenia. Neuronal mechanisms supporting working memory under normal conditions have been described and include persistent, high-frequency activity of prefrontal cortical neurons. However, little is known about the molecular and cellular basis of working memory dysfunction in the context of neuropsychiatric disorders. To elucidate synaptic and neuronal mechanisms of working memory dysfunction, we have performed a comprehensive analysis of a mouse model of schizophrenia, the forebrain-specific calcineurin knock-out mouse. Biochemical analyses of cortical tissue from these mice revealed a pronounced hyperphosphorylation of synaptic vesicle cycling proteins known to be necessary for high-frequency synaptic transmission. Examination of the synaptic vesicle cycle in calcineurin-deficient neurons demonstrated an impairment of vesicle release enhancement during periods of intense stimulation. Moreover, brain slice and *in vivo* electrophysiological analyses showed that loss of calcineurin leads to a gene dose-dependent disruption of high-frequency synaptic transmission and network activity in the PFC, correlating with selective working memory impairment. Finally, we showed that levels of dynamin I, a key presynaptic protein and calcineurin substrate, are significantly reduced in prefrontal cortical samples from schizophrenia patients, extending the disease relevance of our findings. Our data provide support for a model in which impaired synaptic vesicle cycling represents a critical node for disease pathologies underlying the cognitive deficits in schizophrenia.

Introduction

Working memory is the active process by which information is maintained in short-term memory stores and manipulated during performance of complex, goal-directed tasks (Baddeley, 2011). Working memory function is known to correlate with sustained, high-frequency firing of neurons and coordinated network activity within the PFC in multiple species (Funahashi et al., 1989; Funahashi et al., 1993), and it is thought that these neuronal activities represent ongoing information maintenance and processing (Goldman-Rakic, 1995). Impaired working memory is associated with a number of CNS disorders, including Alzheimer's disease (Huntley et al., 2011), multiple sclerosis (Calabrese, 2006), major depression (Castaneda et al., 2008), attention deficit hyperactivity disorder (Doyle, 2006), and schizophrenia (Mesholam-Gately et al., 2009). Cognitive impairments associated with schizophrenia comprise a core component of the disease, are a key factor in the inability of patients to integrate into society, and are not effectively treated by current antipsychotic therapies (Kurtz et al., 2008). Despite the importance of cognitive deficits in disease manifestation, the mechanisms underlying working memory impairments in schizophrenia remain poorly understood.

Calcineurin is a calcium-dependent protein phosphatase that regulates a number of neuronal processes, including synaptic transmission and plasticity (Rusnak and Mertz, 2000; Groth et al., 2003). A growing body of evidence suggests a role for calcineurin dysfunction in cognitive impairments in schizophrenia. Genetic association studies of several populations have linked the

Received Nov. 12, 2012; revised April 22, 2013; accepted May 12, 2013.

Author contributions: J.R.C., J.M.L., S.H.K., H.E.G., K.A.R., D.M.R., C.M.H., K.A.W., P.L., M.E.L., T.A.R., and D.J.G. designed research; J.R.C., J.M.L., S.H.K., H.E.G., K.A.R., M.S., B.L., C.J.A., K.A.H., R.J.B., and P.L. performed research; J.R.C., J.M.L., S.H.K., H.E.G., K.A.R., M.S., B.L., D.M.R., C.M.H., K.A.W., and T.A.R. analyzed data; J.R.C., J.M.L., and D.J.G. wrote the paper.

This work was supported by a research and development collaboration with Otsuka Pharmaceutical Co. Ltd., and by National Institutes of Health Grant MH088617 to J.M.L. We thank Dr. Maree Webster and the Stanley Medical Research Institute for generously providing the human brain tissue samples; and Marie Fitzpatrick, Radhia Benmohamed, and Rasheedah Malik for cell culture generation and additional technical assistance.

J.R.C., K.A.R., C.M.H., R.J.B., D.M.R., P.L., M.E.L., and D.J.G. are employees and stockholders of Galenea. M.S., B.L., C.J.A., K.A.H., and K.A.W. are stockholders of Galenea. T.A.R. is a consultant and stockholder of Galenea.

*J.R.C. and J.M.L. contributed equally to this work.

Correspondence should be addressed to Dr. David J. Gerber, 50C Audubon Road, Wakefield, MA 01880. E-mail: dgerber@galenea.com.

S. H. Kim's present address: Neurodegeneration Control Research Center, Age-Related and Brain Disease Research Center, Department of Neuroscience, School of Medicine, Kyung Hee University, Seoul, South Korea.

DOI:10.1523/JNEUROSCI.5362-12.2013

 0270-6474/13/3310938-12$15.00/0

occurrence of schizophrenia with genetic variations in *PPP3CC*, the gene encoding the γ isoform of the calcineurin catalytic subunit (Gerber et al., 2003; Horiuchi et al., 2007; Liu et al., 2007). Moreover, specific *PPP3CC* haplotypes were found to be associated with the cognitive deficits in schizophrenia in one of the studies (Liu et al., 2007). Forebrain-specific calcineurin knockout (CN-KO) mice were previously shown to have a spectrum of behavioral abnormalities relevant to schizophrenia, including a severe and selective deficit in working memory (Zeng et al., 2001; Miyakawa et al., 2003). Previous functional analyses of these mice focused on correlating spatial working memory deficits with alterations in hippocampal physiology (Zeng et al., 2001). However, because dysfunction of the PFC is thought to underlie cognitive deficits in schizophrenia (Weinberger et al., 1994), we hypothesized that the selective working memory impairment in the CN-KO mice results from disruption of a cortical synaptic mechanism.

Here, we describe results of our analyses of the molecular, cellular, network, and behavioral consequences of the loss of calcineurin function in cortical neurons. Our results provide evidence for a novel mechanism of working memory dysfunction in which an inability of synapses to rapidly and efficiently mobilize and cycle synaptic vesicles leads to disruptions of high-frequency synaptic and network activities in PFC that are necessary to support working memory. We provide further evidence for this disease mechanism by demonstrating that levels of dynamin I, a key presynaptic protein and calcineurin substrate, are significantly reduced in PFC in schizophrenia patients.

Materials and Methods

Animal use. All experimental procedures were performed in accordance with the National Institutes of Health Guide for the Care and Use of Laboratory Animals. In addition, all experimental procedures and protocols were reviewed and approved for use by the Galenea Institutional Animal Care and Use Committee.

CN knock-out mice. The forebrain-specific calcineurin knock-out mice used in this study were previously described (Zeng et al., 2001). In these mice, the postnatal forebrain-specific knock-out of the *Ppp3r1* gene encoding the calcineurin regulatory subunit protein is achieved by using a transgenic mouse line (CW2 line) in which Cre recombinase is driven by the CaMKII promoter (CaMKII-Cre). In the present work, for most experiments, control animals were homozygous floxed *Ppp3r1* mice. For *in vivo* EEG experiments, homozygous and heterozygous floxed *Ppp3r1* mice were used as controls. Heterozygous forebrain-specific *Ppp3r1* knock-out mice (CN-Het) and homozygous forebrain-specific *Ppp3r1* knock-out mice (CN-KO) were generated by breeding male homozygous floxed *Ppp3r1* mice with female mice that were heterozygous for the floxed *Ppp3r1* allele and the CaMKII-Cre transgene.

Transcript profiling. Transcript profiling was performed on RNA isolated from the PFC of control and CN-KO mice from two separate cohorts consisting of 10 animals per group and 14 animals per group, respectively. Mice were anesthetized with isoflurane, killed by decapitation and brains were rapidly removed. To dissect the PFC region, cuts were made on the medial side of both hemispheres at approximately bregma 2 and interaural 3. This brain region includes all or parts of frontal association cortex, orbital cortex, motor cortex, prelimbic cortex, insular, and cingulate cortex. Brain tissue was stored in RNAlater (QIAGEN) at 4°C. RNA was isolated using RNeasy Mini Kit (QIAGEN) according to the manufacturer's instructions, and concentration and quality were determined with a Bioanalyzer (Agilent Technologies). cRNA probes were synthesized with a 3′ IVT kit (Affymetrix) and profiled using mouse genome 430 2.0 microarrays (Affymetrix), according to the manufacturer's instructions. Robust Multichip Averaging was used to perform background subtraction, normalization, and probe set summarization to obtain an average intensity signal for each probe set on the microarray (Irizarry et al., 2003). For group comparison, Student's *t* test was applied to the data, and Benjamini-Hochberg multiple test correction was applied with a false discovery rate (FDR) cutoff of 0.10.

Western blotting. Cerebral cortices from control or CN-KO mouse brains were dissected and homogenized in ice-cold RIPA buffer, including protease inhibitors plus EDTA (Roche). Homogenates were centrifuged at 15,000 × *g* for 15 min at 4°C, and supernatants were harvested. A total of 20 μg of protein from each homogenate was resuspended into 13 μl of 1× NuPAGE running buffer (Invitrogen). Samples were heated to 70°C for 10 min, loaded onto and run on a 4%–12% Bis-Tris NuPAGE gel, and transferred to nitrocellulose filter paper with a Trans-Blot SD SemiDry Electrophoretic Transfer Cell (Bio-Rad). Western blots were blocked for 1 h at room temperature in 10% milk/TBS and then incubated in primary antibody at 4°C overnight in 5% milk/TBS-T (i.e., 0.1% Tween 20). Blots were rinsed 3 times for 10 min each in TBS-T and incubated in HRP-conjugated secondary antibodies against mouse IgG (Santa Cruz Biotechnology; 1:5000), rabbit IgG (Santa Cruz Biotechnology; 1:5000), or sheep IgG (Abcam; 1:5000) for 1 h in 5% milk/TBS-T. Blots were washed in TBS-T two times for 10 min each and in TBS for 10 min. Blots were developed with chemiluminescence substrate (Western Lightning; PerkinElmer) and exposed on a UVP Biochemi. Phospho-specific antibodies used were as follows: sheep anti-pS774 dynamin I (Abcam; 1:1000), sheep anti-pS778 dynamin I (Abcam; 1:1000), rabbit anti-pS795 dynamin I (Santa Cruz Biotechnology; 1:200), rabbit anti-pS9 synapsin I (Cell Signaling Technology; 1:1000), rabbit anti-pS62/67 (Novus Biologicals; 1:1000), rabbit anti-pS551 (Novus Biologicals; 1:1000), and rabbit anti-pS645 PIP5K1γ (custom generated and purified by Open Biosystems). Total protein antibodies were as follows: mouse anti-dynamin I (Santa Cruz Biotechnology; 1:200), mouse anti-synapsin I (Synaptic Systems; 1:1000), and mouse anti-PIP5K1γ (BD Biosciences; 1:250). Western blots were repeated on at least two different sets of control and CN-KO cerebral cortex proteins for each antibody.

Synaptic vesicle cycling assays. For calcineurin shRNA assays, hippocampal CA3-CA1 regions were dissected from 2-d-old Sprague Dawley rats, dissociated, and plated onto poly-ornithine-coated glass for 14–21 d as previously described (Ryan, 1999). All constructs were transfected 8 d after plating. Experiments were performed 14–21 d after plating (6–13 d after transfection), and the coverslips were mounted in a rapid-switching, laminar-flow perfusion and stimulation chamber (volume ~75 μl) on the stage of a custom-built laser illuminated epifluorescence microscope. Live cell images were acquired with an Andor iXon+ (model DU-897E-BV) back-illuminated EMCCD camera in epifluorescence. A solid-state diode pumped 488 or 532 nm laser shuttered using Acousto-Optic Tunable Filters in all not data acquiring periods served as a common light source for the setup. Fluorescence excitation and collection were performed through a 40× 1.3 NA Fluar Zeiss objective using 515–560 nm emission and 510 nm dichroic filters. Action potentials were evoked by passing 1 ms current pulses, yielding fields of ~10 V/cm via platinum-iridium electrodes. Cells were continuously perfused (0.2 ml/min) in a saline solution containing (in mM) 119 NaCl, 2.5 KCl, 2 $CaCl_2$, 2 $MgCl_2$, 25 HEPES (buffered to pH 7.4), 30 glucose, 10 μM CNQX, and 50 μM D,L-2-amino-5-phosphonovaleric acid (AP5). Temperature was clamped at 30°C to minimize effects from temperature fluctuation. For pharmacological calcineurin inhibition assays in cortical cultures, cultures were generated and experiments were performed as previously described (Hempel et al., 2011).

Multielectrode array slice electrophysiology. All solutions used for preparation and acute culture were carboxygenated (95%/5% O_2/CO_2). Control, CN-Het, or CN-KO mice were anesthetized with isoflurane and killed by rapid decapitation, and brains were harvested and immediately placed in ice-cold chopping saline (CS; 110 mM sucrose, 60 mM NaCl, 3 mM KCl, 1.25 mM NaH_2PO_4, 28 mM $NaHCO_3$, 0.5 mM $CaCl_2$, 7 mM $MgCl_2$, 5 mM D-glucose, and 0.6 mM ascorbate). Sagittal cuts were made to remove the lateral-most one-third of the brain from each hemisphere. The cerebellum was removed before hemisectomy. The two halves of the brain were secured to a cutting block (VetBond), medial side up. Sagittal slices (400 μm) were isolated using a vibratome (Vibratome). Freshly isolated slices were immediately transferred to a room temperature equilibration buffer consisting of 50% CS and 50% artificial CSF (aCSF; 124 mM NaCl, 3 mM KCl, 1.25 mM NaH_2PO_4, 36 mM $NaHCO_3$, 2 mM $CaCl_2$,

Table 1. Human PFC samples cohort information[a]

	n	Male	Female	Age (yr)	PMI (hr)	Duration (yr)	Fluphenazine equivalents (mg)	pH	Store (days)
Normal	14	9	5	49 ± 11	22.2 ± 9.4	—	—	6.28 ± 0.21	318 ± 213
Schizophrenia	11	6	5	48 ± 13	34.4 ± 14.2	24 ± 13	55,900 ± 69,101	6.28 ± 0.20	587 ± 250
Bipolar	12	7	5	42 ± 12	30.9 ± 16.2	19 ± 10	23,158 ± 25,432	6.28 ± 0.14	585 ± 173

[a]Human schizophrenia, bipolar disorder, and control PFC (Brodmann area 46) samples from the Stanley Neuropathology Consortium were obtained from the Stanley Medical Research Institute. Fifteen samples were obtained from each group. To ensure high-quality protein samples, brain tissues with reported pH <5.5 were removed from analysis. Shown are the cohort statistics from the remaining samples.

1 mM $MgSO_4$, and 10 mM D-glucose). After completion of slice isolation, slices were allowed to equilibrate for 20 min before transfer to 100% aCSF at room temperature. Slices were further equilibrated for 45 min in 100% aCSF at room temperature before experimentation.

Slices were transferred to a perforated, multielectrode array (200/30 array, Multichannel Systems). aCSF was perfused into the chamber at 2 ml/min, and an in-line heater maintained solution temperatures in the chamber at 30°C. Gentle suction (200 μl/min) was applied underneath the slice. Slices were allowed to equilibrate to the chamber for 15 min before further experimentation. The chamber was electrically grounded via an internal circuit on the perforated array and a silver-chloride plug connected to the amplifier. Extracellular potentials were recorded using 59, 30-μm-diameter disc electrodes placed in an 8 × 8 array. Electrical signals were bandpass filtered by the amplifier (0.1 Hz-10 kHz), digitized at 10 kHz, and stored on a PC. Each electrode could be independently set to record electrical potentials or deliver electrical stimuli.

For paired pulse ratio experiments, slices were stimulated at a voltage that yielded fEPSPs with a left slope that was half the maximum that could be evoked. Paired stimuli were administered with interstimulus intervals at 20, 50, 100, 200, and 300 ms. Ratios were expressed as the slope of the second response divided by the slope of the first response. Responses were averaged over all electrodes that exhibited robust fEPSPs within 3–6 ms of stimulus onset.

For synaptic fatigue experiments, slices were maintained in aCSF that also contained picrotoxin (10 μM) and AP5 (10 μM). Stimuli were delivered at intensities that evoked 75% of the maximal response for a particular slice. Basal synaptic efficacy was monitored for 2 min (0.2 Hz) before and 15 min after induction of synaptic fatigue. Synaptic fatigue was induced by administering 2000 stimuli delivered at 20 or 40 Hz. Electrical stimuli were delivered as 100 μs square waves. When multiple electrode sites within a defined brain region (e.g., PFC) were monitored in conjunction with a single site of stimulation on a particular slice, data from recording electrode sites were averaged and one dataset was considered per slice, per experiment.

Input/output (I/O) relationships were determined by stimulating slices with a range of stimulus intensities (0.5–4.5 V) and recording fiber volley amplitude (μV) and fEPSP left slope (V/s) for each stimulus. I/O curves were constructed by averaging all responses over discrete fiber volley amplitude ranges to determine average fEPSP slopes. Data were fit with second-order quadratics, and an *F* test was used to determine whether curves were significantly different.

For neural oscillation analysis, sagittal PFC slices were generated and positioned on the MEA as above. Spontaneous activity was continuously recorded at 5 or 10 kHz during this experiment. Baseline activity was monitored for 10 min before induction of oscillations. Neural oscillations were evoked by addition of carbachol (20 μM) to the aCSF for 20 min. Carbachol was then washed out, and spontaneous activity was monitored for an additional 20 min. Power analysis of signals was performed in 1 min bins using a Fourier transform with a Hamming window and a spectral resolution of ~1 Hz. Power during neural oscillations was analyzed using a two-way ANOVA with repeated measures.

In vivo electrophysiology. Control, CN-Het, and CN-KO female mice of 4–5 months of age were used in these experiments. An *in vivo* electrode, including a bundle of 8 tungsten wires, was stereotaxically (from bregma: 2.7 mm rostral, 0.7 mm lateral; from dura: 0.5 mm deep) implanted into mouse PFC using standard rodent surgical procedures. Electrical signals from the electrode bundle were propagated to a multichannel amplifier via a surgically implanted Omnetics connector and a commercially available headstage (Multichannel Systems). Signals were bandpass filtered (1–1000 Hz), digitized, and stored on a computer. Behavior was monitored and recorded using a digital video camera (Logitech). EEGs were analyzed via FFT spectral analysis with Hamming windows. Animals were housed in cages that provided additional headroom for the surgical apparatus with access to food and water *ad libitum*. Animals were allowed to recover from surgery for 1 week before experimentation. During recovery, animals were habituated to the laboratory environment and handling. The headstage was plugged into the Omnetics connector integrated into the headgear, and animals were immediately placed into the recording chamber for 30 min. EEGs were analyzed in the θ (4–9 Hz), γ (30–90 Hz), and ripple (100–300 Hz) frequency bands.

Human brain protein Western blot. Postmortem brain tissue was provided by the Stanley Medical Research Institute and consisted of tissue slices (14 μm thick) from PFC Brodmann area 46 mounted on glass slides from the Neuropathology Consortium of 15 each of control, schizophrenia patient, and bipolar disease patient brain samples. Protein was extracted with 200 μl RIPA buffer plus protease inhibitors (Roche), and tissue extractions were scraped into Eppendorf tubes. Protein was incubated on ice for 20 min and centrifuged for 20 min at 15,000 × *g* at 4°C, and supernatant was isolated. Protein concentrations were determined using a BCA method (Pierce). Samples were run on five separate 12-well 4–12% Bis-Tris NuPAGE gels (Invitrogen). A total of 20 μg of protein from nine samples (three samples from each group) was loaded onto each gel along with one lane of a control cerebral cortex protein extract (Biochain) to act as a normalization control between the multiple gels. Protein was transferred to nitrocellulose, and immunodetection was performed by overnight incubations with mouse anti-dynamin I (Santa Cruz Biotechnology; 1:200) and rabbit anti-β-III-tubulin (Sigma; 1:1000) at 4°C followed by incubations with anti-mouse or anti-rabbit HRP-conjugated secondary antibodies (1:5000; Santa Cruz Biotechnology) for 1 h at room temperature. Western blots were developed on a UVP Biochemi System, and pixel density was determined for each band using LabWorks 4.6. To control for protein loading within the gel, the pixel density for each protein was normalized to the β-III-tubulin pixel density within that lane. To control for protein expression across gels, the adjusted dynamin I expression level for each brain sample was normalized to the adjusted dynamin I expression level in the control sample lane of the same gel. Because of the known effects of low pH on the quality of postmortem brain tissue (Monoranu et al., 2009), samples with a reported pH <5.5 were removed from analyses. Cohort information for the final sample set is presented in Table 1. All Western blots and analyses were performed by individuals blinded to the sample group identities.

Behavioral assays. For behavioral analyses, control, CN-Het and CN-KO mice were used as subjects. Mice were between 3 and 6 months of age at the time of testing. The mice were group housed in ventilated cages with corncob bedding and were maintained on a 12 h light-dark cycle. Animals had free access to water and food. Passive avoidance testing was performed as described previously (Wiig et al., 2009).

Delayed nonmatch to position (DNMTP) testing was performed essentially as described previously (Wiig and Burwell, 1998). Mice were food-restricted to 90% of their free feeding body weight. Testing was conducted in operant testing chambers (Coulbourn Instruments) interfaced with a PC and controlled by a Coulbourn Graphic State Notation software package. Operant chambers had Plexiglas side walls and a floor constructed of steel rods. On the front wall of the test chamber were two retractable levers. A food hopper for dispensing sweetened condensed milk was located halfway between the two retractable levers. Stimulus lights were located above both levers and the food hopper. On the back wall was a nose-poke hole. A partially shaded house light was used to illuminate the chamber during the time-out trials. The operant chamber

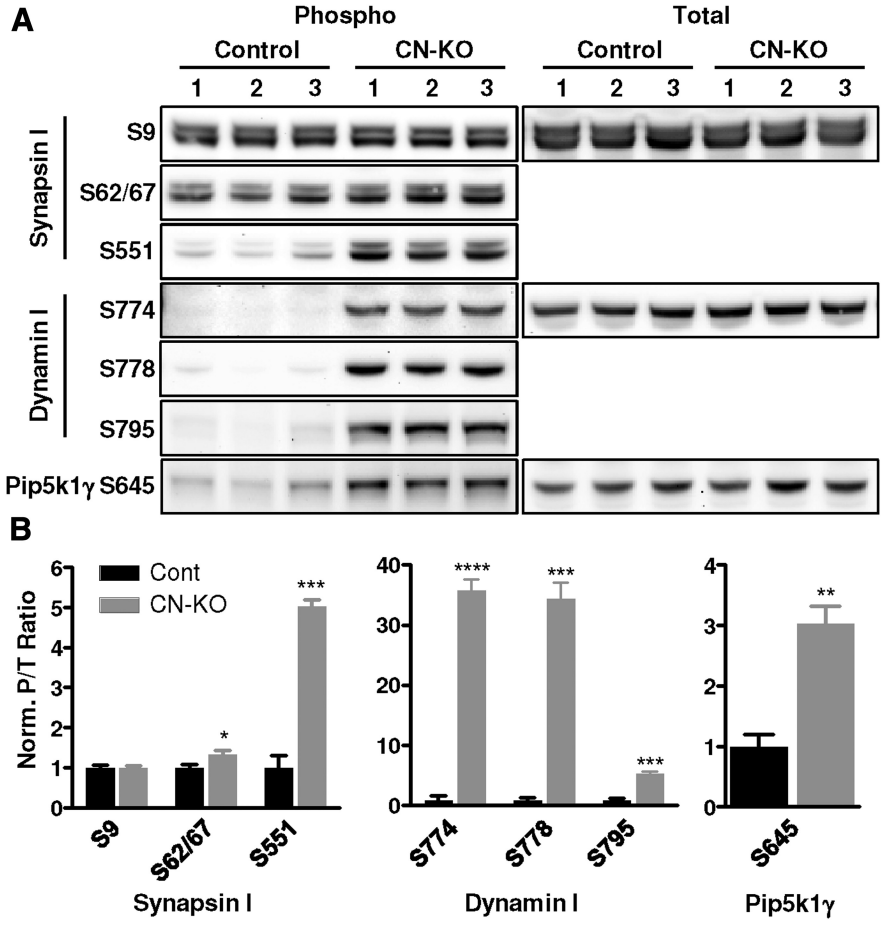

Figure 1. Synaptic vesicle cycling proteins are hyperphosphorylated in CN-KO cortex. ***A***, Western blotting was performed on cerebral cortex protein extracts from three control and three CN-KO mice. Protein was probed with antibodies against total and phosphorylated dynamin I (Dnm1), synapsin I (Syn1), and Pip5k1γ (Pip5k1c) at the indicated residues. Densitometry analysis was performed. ***B***, Mean (±SEM) phospho:total band densitometry ratios, normalized to mean ratio of control bands. $*p < 0.05$. $**p < 0.01$. $***p < 0.001$. $****p < 0.0001$.

was enclosed in a sound-attenuating outer chamber fitted with an exhaust fan. All training was conducted with the house light off, except for time-out periods. The stimulus lights above each lever and the food hopper were illuminated on each presentation of lever or activation of the hopper. Pretraining on the DNMTP task includes four stages. In stage 1, mice were trained to press either the left or the right lever on successive trials. Each lever press was rewarded with sweetened condensed milk (diluted 1:3 with water). In all stages of shaping and training, the intertrial interval was 5 s. In stage 2, mice were trained to nose-poke at the back of the chamber when the cue light inside the nose-poke hole was on to gain access to the levers. Both levers were extended immediately after the nose-poke, and a response on either lever was reinforced. In stage 3, either the left or the right lever was presented and was retracted when pressed. The lever press resulted in the illumination of the nose-poke hole. A nose-poke then produced extension of both levers, and a press on either lever was reinforced. The first stage of training began once all mice had learned the complete chain of responses. The extension of the single lever at the beginning of the trial constituted the sample phase, and the extension of both levers after the intervening nose-poke constituted the choice phase. The choice was presented immediately after the nose-poke without delay. Mice were rewarded for choosing the lever that was not pressed during the sample phase. An incorrect (error) response resulted in a 5 s time-out, in which the house-light was illuminated. Mice were trained on this stage until all mice had achieved a criterion of 70% correct. The second DNMTP stage of training was identical to the previous stage, except that a selected delay interval was interposed between presentation of the sample and choice phases of the task. Mice were first trained on short delay protocols until they had reached a criterion of 75% correct over two consecutive days. Once the criterion had been reached, they were moved onto a delay protocol incorporating slightly longer delays. Using this procedure, they were gradually shaped until they were able to perform on a final delay protocol of 0, 2, 4, 6, 8, and 10 s. Mice were given 100 trials per session and one session on each of 5 d per week. Dependent variables were the number of trials taken to reach criterion, the number of completed trials within each session, and percentage correct on the testing sessions. Data were analyzed using independent *t* tests.

Results

Loss of calcineurin impairs high-frequency presynaptic function

To determine the functional effects of calcineurin loss in cortical neurons, we performed a series of analyses of forebrain-specific calcineurin knock-out mice (Zeng et al., 2001). We first confirmed that expression of the *Ppp3r1* gene encoding the calcineurin regulatory subunit is disrupted in PFC in these mice by performing transcript profiling on PFC tissue isolated from the mice. Transcript profiling results from two separate cohorts of CN-KO mice confirmed reduced expression of the *Ppp3r1* gene in CN-KO relative to control PFC (first cohort, 3.7-fold average reduction, FDR $\leq 4.6 \times 10^{-5}$; second cohort, 2.9-fold average reduction, FDR $\leq 1.9 \times 10^{-5}$). Residual expression likely results from inclusion of CaMKII-negative cells in the tissue samples (e.g., inhibitory neurons, glia, and blood vessels). These results were confirmed by qRT-PCR (data not shown).

Calcineurin dephosphorylates a set of proteins known to be critical for synaptic vesicle cycling (Cousin and Robinson, 2001), likely underlying its positive modulation of this process (Cousin and Robinson, 2001; Sun et al., 2010). A number of reports have indicated a requirement for these presynaptic calcineurin substrates in regulating sustained, high-frequency neuronal activity (Cremona et al., 1999; Di Paolo et al., 2002, 2004; Ferguson et al., 2007; Clayton et al., 2009; Sun et al., 2010), suggesting a role for calcineurin in the range of neuronal activity associated with working memory. To investigate whether cortical presynaptic function is altered in CN-KO mice, we first examined the phosphorylation status of presynaptic calcineurin substrates in the cerebral cortex of these mice using phospho-specific antibodies. We observed a significant hyperphosphorylation of multiple presynaptic calcineurin substrates in cerebral cortex of CN-KO mice relative to control mice, including synapsin I S62/67 ($t_{(4)} = 2.93$, $p < 0.05$) and S551 ($t_{(4)} = 12.10$, $p < 0.001$), dynamin I S774 ($t_{(4)} = 19.59$, $p < 0.0001$), S778 ($t_{(4)} = 12.43$, $p < 0.001$), and S795 ($t_{(4)} = 12.11$, $p < 0.001$), and Pip5k1γ S645 ($t_{(4)} = 5.89$, $p < 0.01$) (Fig. 1). Observed hyperphosphorylation did not result from alterations in total protein levels because no significant alterations in the levels of synapsin I ($t_{(4)} = 0.30$, $p = 0.78$), dynamin I ($t_{(4)} = 1.39$, $p = 0.24$), or Pip5k1γ ($t_{(4)} = 1.09$, $p = 0.34$) were observed in CN-KO mice samples. In contrast, there was no

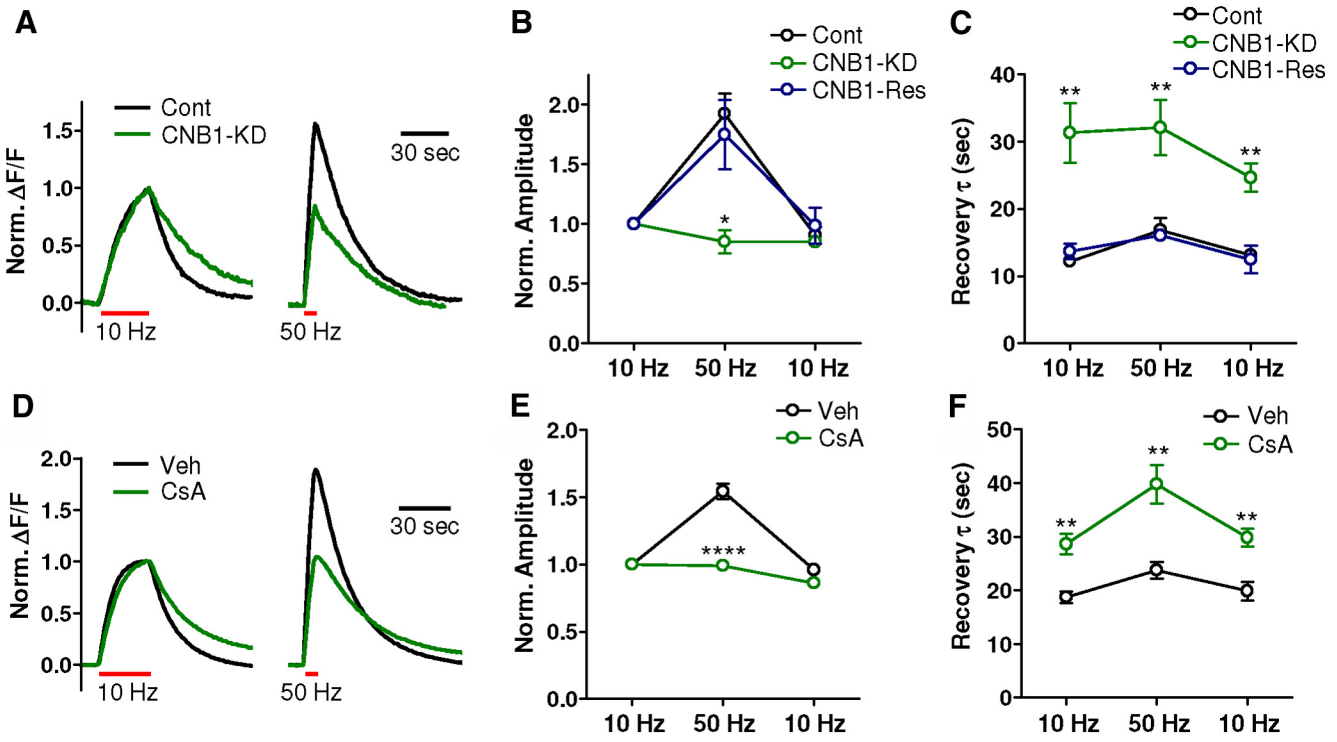

Figure 2. Synaptic vesicle cycling is impaired after knockdown of calcineurin levels. ***A–C***, Neurons transfected with either (1) vGlut1-pHluorin alone (Cont), (2) vGlut1-pHluorin and an shRNA targeting CNB1 (CNB1-KD), or (3) vGlut1-pHluorin, the CNB1-shRNA, and an shRNA-resistant version of CNB1 (CNB1-Res) were subjected to stimulus trains of 300 pulses delivered at (1) 10 Hz, (2) 50 Hz, and (3) 10 Hz. ***A***, vGlut1-pHluorin fluorescence responses from single neurons to the first 10 Hz and the 50 Hz pulse trains from control neurons and CNB1-shRNA transfected neurons. ***B***, Mean (±SEM) response amplitudes normalized to the response of the first 10 Hz stimulus train from control ($n = 5$), CNB1-shRNA ($n = 5$), and CNB1-shRNA rescued ($n = 4$) neurons. ***C***, The vGlut1-pHluorin waveform decays were fit with a single-exponential decay curve. Shown are the mean (±SEM) recovery time constants from control ($n = 5$), CNB1-shRNA ($n = 5$), and CNB1-shRNA rescued ($n = 4$) neurons. ***D–F***, Primary rat cortical neurons expressing the synaptophysin-pHluorin reporter delivered by AAV transduction were treated with vehicle (Veh; $n = 5$) or cyclosporin A (CsA, 20 μM; $n = 5$) and analyzed as described above (***A–C***). There was a significant reduction in the amplitude of responses to the 50 Hz stimulus ($t_{(8)} = 8.63$, $p < 0.0001$) and a significant increase in the recovery time constant for the 10 Hz stimulus 1 ($t_{(8)} = 4.39$, $p < 0.01$), the 50 Hz stimulus ($t_{(8)} = 4.13$, $p < 0.01$), and the 10 Hz stimulus 2 ($t_{(8)} = 4.17$, $p < 0.01$) in cyclosporin A-treated versus vehicle-treated neurons. *$p < 0.05$. **$p < 0.01$. ****$p < 0.0001$.

change in phosphorylation of a site on synapsin I (S9) that is not a substrate for calcineurin (Jovanovic et al., 2001) (Fig. 1; $t_{(4)} = 0.17$, $p = 0.87$). These data indicate that loss of calcineurin function in the cerebral cortex has a major impact on the phosphorylation status of presynaptic regulatory proteins, either directly or indirectly through modulation of other phosphatases, and suggest that presynaptic function is altered in the cerebral cortex of CN-KO mice.

We next directly assessed the impact of loss of calcineurin function on synaptic vesicle mobilization and recycling during high-frequency activity. We used the vGlut1-pHluorin optical reporter to measure synaptic vesicle cycling in cultured hippocampal neurons in which calcineurin function was impaired by introduction of a shRNA targeting the calcineurin regulatory subunit CNB1 (Kim and Ryan, 2010). Neurons were stimulated with three trains of 300 pulses delivered at 10 Hz, at 50 Hz, and again at 10 Hz. In control neurons, there was an ~2-fold increase in the response amplitude to the 50 Hz stimulus relative to the first 10 Hz stimulus, indicating a higher rate of synaptic vesicle mobilization and exocytosis at the higher frequency (Fig. 2*A*,*B*). In CNB1-knockdown neurons, there was a significant reduction in the amplitude increase in response to 50 Hz relative to 10 Hz trains (Fig. 2*A*,*B*; $n = 5$/group, $t_{(8)} = 5.50$, $p < 0.001$). This effect was eliminated by cotransfection of a cDNA encoding a shRNA-resistant CNB1 transcript (Kim and Ryan, 2010) (Fig. 2*B*; $n = 4$, $t_{(7)} = 0.55$, $p = 0.60$). These data suggest that loss of calcineurin results in an impairment of synaptic vesicle release during high-frequency action potential stimulation. Moreover, in line with recent findings (Sun et al., 2010), the rate of synaptic vesicle endocytosis was slowed after all stimulation trains by CNB1-knockdown (Fig. 2*A*,*C*; 10 Hz train 1, $t_{(8)} = 4.07$, $p < 0.01$; 50 Hz, $t_{(8)} = 3.39$, $p < 0.01$; 10 Hz train 2, control: $t_{(8)} = 4.54$, $p < 0.01$), an effect rescued by cotransfection with the shRNA-resistant CNB1 (Fig. 2*C*; 10 Hz train 1, $t_{(7)} = 0.72$, $p = 0.50$; 50 Hz train, $t_{(74)} = 0.37$, $p = 0.74$; 10 Hz train 2, $t_{(7)} = 0.28$, $p = 0.79$). Critically, vesicle endocytosis has been demonstrated to be a rate-limiting step of synaptic vesicle cycling, with the impact of slowed endocytosis on synaptic transmission being most significant during high-frequency activity (Kavalali, 2006). Although these data were collected in hippocampal neurons, similar results were observed in rat cortical neurons in which calcineurin was pharmacologically inhibited with cyclosporin A (20 μM), and the synaptic vesicle cycle was analyzed using a synaptophysin-pHluorin reporter construct (Granseth et al., 2006; Hempel et al., 2011) (Fig. 2*D–F*). This concentration of cyclosporin A was sufficient to prevent the dephosphorylation of dynamin I S778 induced by addition of 50 mM KCl in cultured rat cortical neurons (data not shown). Collectively, these results indicate that loss of calcineurin function impairs the ability of synapses to mount and maintain synaptic vesicle exocytosis during periods of intense stimulation.

Impaired high-frequency synaptic transmission in the CN-KO and CN-Het mouse PFC

Our observations of impaired synaptic vesicle cycling during intense neuronal activity suggested that high-frequency synaptic

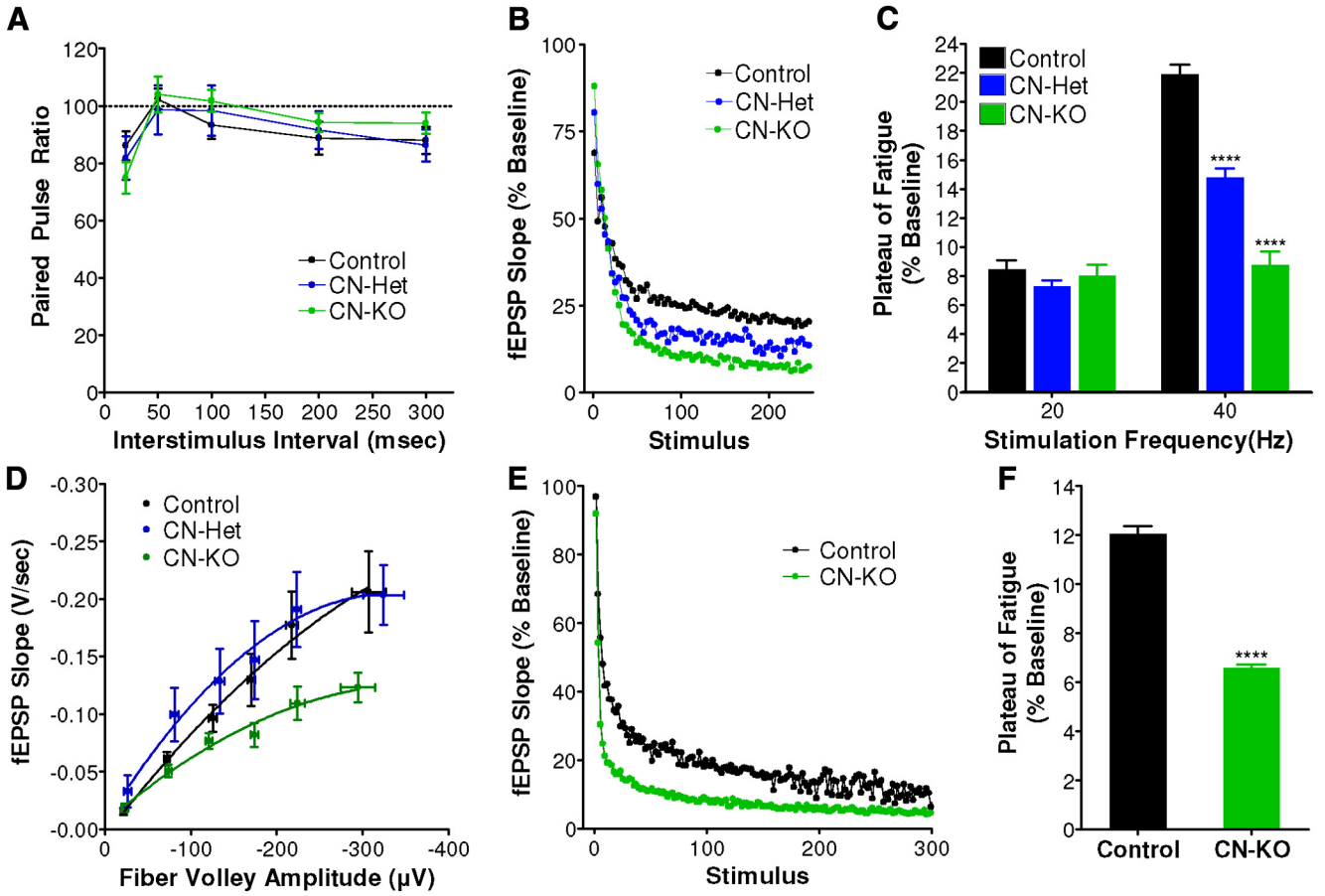

Figure 3. Synaptic fatigue is augmented in the PFC of CN-KO and CN-Het mice. ***A***, Paired pulse ratios were measured in sagittal slices containing PFC from CN-KO ($n = 24$), CN-Het ($n = 5$), and littermate controls ($n = 16$). ***B***, Synaptic fatigue was induced in PFC slices from control ($n = 8$), CN-Het ($n = 5$), and CN-KO ($n = 6$) mice by stimulating at 40 Hz and monitoring the left slope of evoked fEPSPs. ***C***, Synaptic fatigue data from PFC slices stimulated at 20 Hz or 40 Hz were fit with single exponential curves, and the magnitude of fatigue was determined as the plateau of the fit; control ($n = 8$), CN-Het ($n = 5$), CN-KO ($n = 6$). ***D***, Basal synaptic transmission was assessed in PFC by relating fEPSP slope to fiber volley amplitudes in response to a series of electrical stimuli. PFC slices isolated from CN-KO ($n = 24$) animals exhibited lower I/O relationships relative to either CN-Het ($n = 5$) or control ($n = 16$) animals. ***E***, Synaptic fatigue in response to a 40 Hz stimulus train was measured at the mossy fiber synapse in which calcineurin is intact in postsynaptic neurons but deficient in presynaptic terminals of CN-KO mice; CN-KO ($n = 4$), control ($n = 4$). ***F***, Summary data for fatigue experiments in ***E***. ****$p < 0.0001$. Data shown in ***A***, ***C***, ***D***, and ***F*** are mean (±SEM).

transmission might be altered in CN-KO cortical circuits. To directly assess the effects of calcineurin deficiency on high-frequency synaptic transmission in PFC, synaptic fatigue assays were performed on sagittal PFC brain slices from CN-KO animals using a perforated multielectrode array (pMEA) system (Gonzalez-Sulser et al., 2011). Heterozygous knock-out mice (CN-Het) were included in this analysis to examine gene dose-dependency of observed effects. No significant differences were observed in paired pulse ratios measured from CN-KO and CN-Het PFC relative to littermate controls, suggesting that basal presynaptic function in PFC is normal in these animals (Fig. 3*A*; $F_{(2,42)} = 0.09$, $p = 0.91$). When challenged with an extended train (50 s) of 40 Hz stimuli, synaptic transmission decayed to significantly lower plateau potentials in PFC slices from CN-KO and CN-Het mice relative to littermate controls with a gene dose-dependent relationship (Fig. 3*B*,*C*; 40 Hz: $F_{(2,20)} = 84$, $p < 0.0001$). No significant differences were observed in the plateau potentials resulting from stimulation trains at 20 Hz in CN-KO and CN-Het mice relative to controls (Fig. 3*C*; 20 Hz: $F_{(2,20)} = 1$, $p = 0.38$), indicating that the increased synaptic fatigue in PFC of these mice is dependent on the frequency of stimulation. The augmentation of high-frequency synaptic fatigue in PFC of CN-KO and CN-Het animals is consistent with the effects of loss of calcineurin on synaptic vesicle mobilization during periods of high-frequency activity in primary neurons and suggests a critical role for calcineurin in maintenance of high-frequency synaptic transmission in the PFC. Examination of I/O curves revealed a significant diminution of responses in PFC slices isolated from CN-KO but not CN-Het animals (Fig. 3*D*; $F_{(6,166)} = 6.2$, $p < 0.0001$). The decreased responses were not accompanied by a reduction in the fiber volley amplitude ($F_{(2,20)} = 0.47$, $p = 0.63$), suggesting reduced postsynaptic responsiveness in the CN-KO PFC. This reduction in basal synaptic transmission could contribute to the CN-KO behavioral phenotype; however, it does not explain the working memory dysfunction observed in CN-Het animals (see Fig. 5).

The impaired high-frequency synaptic transmission observed in the PFC of CN-KO mice could result from loss of calcineurin at either the presynaptic terminals or postsynaptic spines, or both. To directly determine the impact of loss of presynaptic calcineurin on maintenance of high-frequency synaptic transmission, we measured synaptic fatigue at the hippocampal mossy fiber synapse in CN-KO mice. This synapse permits specific analysis of the consequences of loss of presynaptic calcineurin function on synaptic transmission because *Ppp3r1* gene deletion does not occur in CA3 pyramidal neurons in these mice, leaving intact postsynaptic calcineurin expression at this synapse (Zeng et al., 2001).

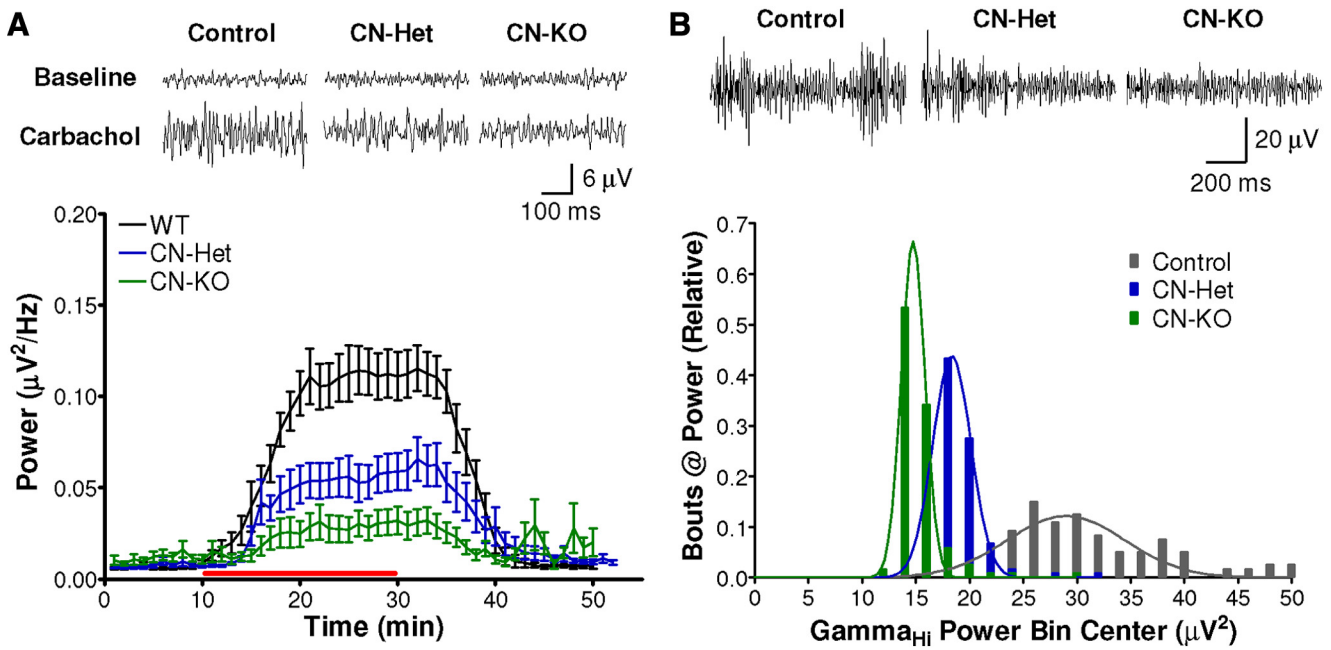

Figure 4. High-frequency oscillatory network activity is impaired in PFC of CN-KO and CN-Het mice. ***A***, Extracellular potentials were recorded in PFC from sagittal slices from CN-KO ($n = 10$), CN-Het ($n = 12$), and littermate control animals ($n = 12$) using a pMEA. Oscillations were evoked with carbachol (red bar, 20 μM). Representative traces above summary data indicate spontaneous activity in the γ band (30–90 Hz) before (Baseline) and after application of carbachol (Carbachol). Data shown are mean (±SEM). ***B***, Neural activity was recorded from the PFC of freely behaving CN-KO ($n = 4$), CN-Het ($n = 20$), and littermate control mice ($n = 16$) during the first 15 min of exposure to a novel environment. Representative traces show $Gamma_{Hi}$ (65–90 Hz) bandpass filtered signals. Summary histogram illustrates the relative number of times a particular level of $Gamma_{Hi}$ power was observed in each animal cohort.

Synaptic fatigue at mossy fiber synapses in response to 40 Hz stimulation was significantly greater in slices derived from CN-KO animals relative to those from littermate controls as indicated by reduced plateau potential (Fig. 3*E*,*F*; $t_{(6)} = 16$, $p < 0.0001$), demonstrating that disruption of presynaptic calcineurin alone results in a severe deficit in maintenance of high-frequency synaptic transmission.

High-frequency network oscillations are disrupted in the CN-KO mouse PFC

Emerging evidence indicates that coherent, high-frequency network activity in the PFC, including synchronous γ oscillatory activity, is critical for working memory and other executive functions mediated by the PFC (Uhlhaas et al., 2008). Moreover, γ oscillations in PFC have been reported to be perturbed in schizophrenia patients, particularly during the performance of working memory tasks (Uhlhaas and Singer, 2010). We hypothesized that the observed deficits in the maintenance of high-frequency synaptic transmission in CN-KO and CN-Het mouse PFC may lead to impaired initiation and/or maintenance of γ oscillations. Oscillatory network activity was measured in sagittal PFC brain slices using the pMEA system (Gonzalez-Sulser et al., 2011). Oscillations were induced with the general cholinergic receptor agonist, carbachol (20 μM), and data were bandpass filtered to isolate γ oscillations (30–90 Hz). The power of carbachol-induced γ oscillations in PFC brain slices from CN-KO and CN-Het mice was significantly reduced relative to that of slices from littermate control animals (Fig. 4*A*; $F_{(2,1320)} = 13$, $p < 0.0001$). Moreover, the observed reductions in maximum oscillatory power were calcineurin gene dose-dependent (Fig. 4*A*). These data indicate that isolated PFC neural networks in the CN-KO mouse are deficient in the ability to generate high-frequency oscillatory activity induced by cholinergic stimulation.

To determine whether the deficits we observed in isolated PFC circuitry extend to intact, connected networks *in vivo*, we implanted microwire bundle electrodes in the PFC of CN-KO, CN-Het, and littermate control mice and recorded neural activity from the PFC of freely behaving animals. Novelty exploration in rodents is associated with robust activation of multiple neurotransmitter systems in the PFC, including the cholinergic system (Leussis and Bolivar, 2006). Therefore, we measured the power of oscillations in the $Gamma_{Hi}$ frequency band (65–90 Hz) in PFC upon placement of mice into a novel environment to elicit PFC network activity. Consistent with our findings *in vitro*, γ oscillations evoked in the PFC *in vivo* by exposure to a novel environment exhibited a calcineurin gene dose-dependent impairment (Fig. 4*B*; $F_{(2,39)} = 535$, $p < 0.0001$). *Post hoc* analyses using the Newman–Keuls test indicated that the power of $Gamma_{Hi}$ oscillatory activity recorded from the PFC of littermate control mice was significantly higher than that of CN-Het (Fig. 4*B*; $q_{(37)} = 41$, $p < 0.0001$) and CN-KO animals (Fig. 4*B*; $q_{(37)} = 33$, $p < 0.0001$). Collectively, these data indicate that loss of calcineurin results in a severe disruption in coherent network activity in the PFC, consistent with the impaired high-frequency synaptic function observed in these mice.

Nonspatial working memory is impaired by genetic reduction of calcineurin levels

Previous examination of cognitive function in CN-KO mice revealed a selective and severe impairment in spatial working/episodic-like memory as assessed in delayed match-to-place water maze and eight-arm radial maze tasks (Zeng et al., 2001). To extend the behavioral analysis to a working memory task that does not depend on distal spatial cues and to examine gene dose-dependency of cognitive effects, we analyzed CN-KO and CN-Het mice for performance in a DNMTP task.

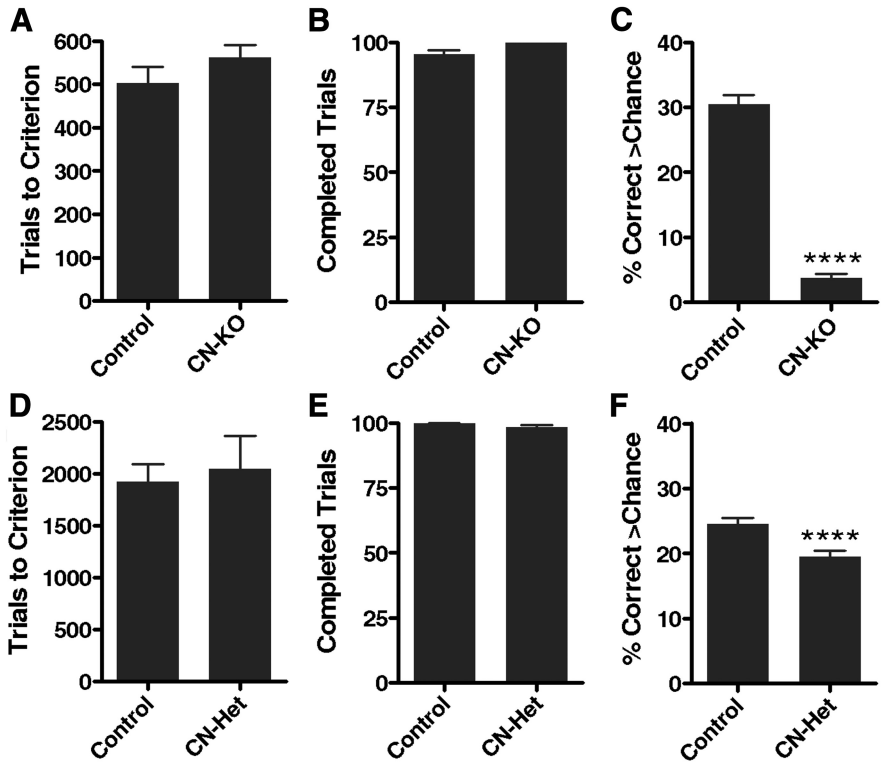

Figure 5. CN-KO and CN-Het mice have impaired performance in the DNMTP task. The performance of CN-KO and CN-Het mice was analyzed in a DNMTP working memory task. ***A***, ***D***, Mean (±SEM) number of trials for mice to reach criterion for basic performance of the task with no imposed delay. ***B***, ***E***, Mean (±SEM) number of completed trials per test session. ***C***, ***F***, Mean (±SEM) percentage correct above chance on the DNMTP task after imposition of delays within the task. ****$p < 0.0001$.

DNMTP is an operant conditioning task in which the animal initially presses a lever (sample phase), and after a brief delay period, uses the information in combination with a set of rules to ultimately press a second lever (test phase) with the goal of receiving a food reward (Wiig and Burwell, 1998). The CN-KO mice were capable of learning the rules governing the DNMTP task, as there were no significant differences from control mice in trials to achieve criterion with no delay between the sample and test phases (Fig. 5*A*; $n = 6$/group, $t_{(8)} = -1.65$, $p = 0.28$). As delays were introduced between the sample and test phases, the performance of CN-KO mice decreased to near chance levels representing a significant deficit relative to littermate controls (Fig. 5*C*; $n = 6$/group, $t_{(189)} = 17.49$, $p < 0.0001$). CN-Het mice were capable of completing the task with imposed delays, but their performance was significantly impaired relative to littermate controls (Fig. 5*F*; $n = 8$/group, $t_{(276)} = 4.36$, $p < 0.0001$). Similar to CN-KO mice, CN-Het mice exhibited no differences in the acquisition of operant sequencing (Fig. 5*D*; $n = 8$/group, $t_{(14)} = -0.35$, $p = 0.73$). The deficits in both groups did not appear to result from motivational or other factors unrelated to working memory because all groups completed >98% of trials (Fig. 5*B*,*E*). No deficits in performance of a passive avoidance task were observed in CN-KO and CN-Het mice, supporting previous results indicating that reference memory is normal in these mice (data not shown). Collectively, these results confirm and extend the demonstration of severe and selective cognitive impairment in CN-KO mice. In addition, the greater magnitude of the working memory deficit in the CN-KO versus the CN-Het mice relative to control mice suggests a gene dose-dependent relationship between calcineurin disruption and working memory performance.

Reduced dynamin I protein in schizophrenia PFC

Our observations in the CN-KO mouse model suggest that disruptions in synaptic vesicle cycling may be relevant to cognitive deficits in schizophrenia patients. Indeed, several genomic and proteomic profiling studies have indicated alterations in brain expression of presynaptic proteins in schizophrenia (Faludi and Mirnics, 2011). To specifically investigate alterations in the synaptic vesicle cycling machinery, we measured levels of dynamin I in postmortem PFC brain samples from schizophrenia and bipolar disorder patients and from normal controls (Table 1). Dynamin I is a critical component of the synaptic vesicle endocytosis machinery and a known substrate for calcineurin (Ferguson and De Camilli, 2012). There was a significant reduction in the level of dynamin I protein in PFC samples isolated from patients with schizophrenia ($n = 11$; $t_{(23)} = 2.94$, $p < 0.01$), but not bipolar disorder ($n = 12$; $t_{(24)} = 1.73$, $p = 0.09$), relative to samples from normal controls ($n = 14$) (Fig. 6). The reduction in dynamin I expression observed in PFC of schizophrenia patients supports the concept that perturbations in synaptic vesicle cycling in PFC neurons may represent a contributing factor in cognitive deficits associated with schizophrenia.

A presynaptic model for working memory dysfunction

Results of our analyses of synaptic and network function in the CN-KO cortex suggest a presynaptic mechanism for working memory deficits (Fig. 7). In this model, calcineurin deficiency results in an inability of neurons in PFC to efficiently mobilize and recycle synaptic vesicles during periods of high-frequency activity. This synaptic functional deficit in turn leads to a disruption of the high-frequency neuronal and network activities in PFC that are required for normal working memory function. Our finding of reduced dynamin I expression in PFC from schizophrenia patients suggests that the model is relevant to working memory deficits in schizophrenia and indicates that additional molecular mechanisms may converge on the synaptic vesicle cycle.

Discussion

We have performed a detailed analysis of the molecular, cellular, network, and behavioral effects of loss of cortical calcineurin function, focusing on the CN-KO mouse, a genetic model that recapitulates multiple behavioral alterations in schizophrenia, including selective cognitive deficits. We demonstrate that the status of key synaptic vesicle cycling proteins is significantly altered in the cortex of CN-KO mice. We further demonstrate that calcineurin function is required for efficient synaptic vesicle cycling during high-frequency activity and that calcineurin loss results in gene dose-dependent disruptions of high-frequency

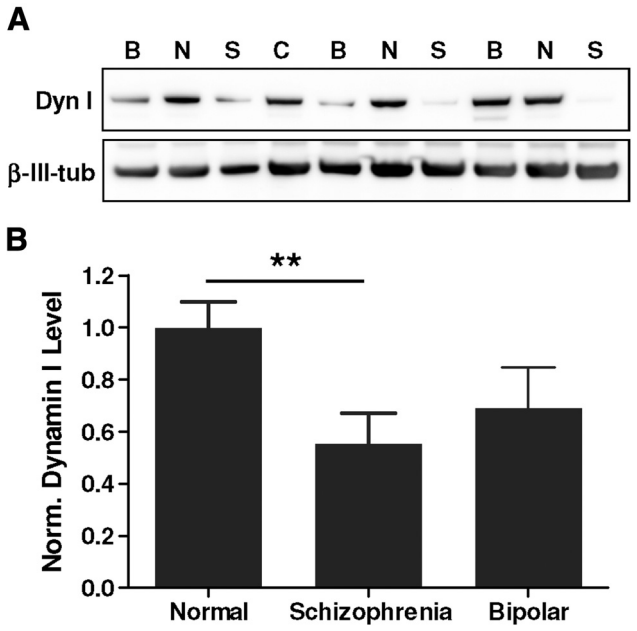

Figure 6. Levels of the synaptic vesicle cycling protein dynamin I are reduced in schizophrenia PFC. Western blotting was performed for dynamin I and β-III-tubulin on protein extracts generated from slices of PFC (Brodmann's area 46) from control individuals ($n = 14$) and from patients with schizophrenia ($n = 11$) or bipolar disease ($n = 12$). (See Table 1 for cohort information.) ***A***, Representative Western blot showing dynamin I and β-III-tubulin expression from normal (N), schizophrenia (S), and bipolar (B) brain samples; C indicates a normalization control consisting of a commercial human cerebral cortex sample. ***B***, Mean (±SEM) dynamin I protein levels measured and calculated as described in Materials and Methods. $^{**}p < 0.01$.

synaptic transmission and neural network oscillations in PFC. Moreover, we show that calcineurin deficiency results in a gene dose-dependent impairment of performance in a DNMTP operant working memory task. Last, we provide evidence that a similar alteration in synaptic vesicle cycling may occur in the PFC of schizophrenia patients as a consequence of reduced expression of the presynaptic protein and calcineurin substrate, dynamin I, which has been shown to be specifically required for sustaining high-frequency neuronal firing (Ferguson et al., 2007). Based on these data, we propose a presynaptic mechanistic framework for working memory dysfunction in the context of schizophrenia (Fig. 7).

Classic experiments in nonhuman primates have shown that neurons in PFC fire persistently at high frequency during delay phases of working memory tasks (Goldman-Rakic, 1990). More recent studies have extended the original characterization of these delay neurons in PFC by adding the concept that coherent, high-frequency γ oscillations in PFC are required for working memory (Uhlhaas et al., 2008). Moreover, there is evidence that sustained periods of transmitter release are necessary for neural networks to support coherent, high-frequency oscillations (Bartos et al., 2007). However, the specific molecular and synaptic mechanisms required for high-frequency neuronal and network activities underlying working memory have not been well defined.

Our results indicate that, during bouts of high-frequency activity in PFC, activation of calcineurin enhances multiple steps of the synaptic vesicle cycle. This enhancement likely results from the dephosphorylation of a set of known calcineurin substrates, termed the dephosphins, that regulate vesicle endocytosis (Cousin and Robinson, 2001) and of other known presynaptic substrates, such as synapsin I (Jovanovic et al., 2001). According to our proposed model, by increasing the availability of vesicles during periods of high-frequency activity, calcineurin functions to maintain synaptic transmission and permits ensembles of neurons to engage in higher-order oscillatory activity. Reduction of calcineurin function attenuates synaptic vesicle cycling, specifically during periods of intense activity, resulting in a selective disruption of the high-frequency firing and oscillatory network activities that are necessary to support higher cognitive processes including working memory.

We have demonstrated a correlation between altered synaptic vesicle cycling and working memory dysfunction in the CN-KO mouse model of schizophrenia. It is important to note that alterations in synaptic vesicle cycling may contribute to the other behavioral abnormalities previously observed in these animals that recapitulate positive and negative symptoms of schizophrenia (Miyakawa et al., 2003). Moreover, calcineurin is known to regulate a number of different aspects of neuronal function in addition to presynaptic vesicle cycling, including postsynaptic receptors, ion channels, gene transcription, and various signal transduction pathways (Groth et al., 2003). A previous characterization of these mice revealed impaired bidirectional synaptic plasticity at hippocampal Schaffer collateral synapses (Zeng et al., 2001), which may play a role in the spatial components of working memory dysfunction in these mice. In addition, in the present study, we observed a reduction in basal synaptic transmission in CN-KO PFC. Because this effect was not present in CN-Het PFC, it is likely not the core mechanism whereby calcineurin deficiency results in the observed deficits in both the CN-Het and CN-KO animals. However, this effect could contribute to the severity of the phenotype observed in CN-KO mice.

Although our study focused on neuronal mechanisms, it is possible that knock-out of calcineurin specifically in neurons may affect the function of other cell types within the brain, such as glia, and thereby contribute to the synaptic functional and behavioral abnormalities observed in the CN-Het and CN-KO mice. It is also possible that the presence of the CaMKII-Cre transgene in the CN-KO and CN-Het mice may contribute to the results demonstrated here. Additional studies are warranted to examine these potential factors in relation to the results described here.

Calcineurin is known to regulate additional elements of the synaptic vesicle cycle that may be involved in the deficits that we observed after its inhibition. A recent report indicated that loss of calcineurin function results in a reduced recycling vesicle pool size and exocytosis kinetics (Kim and Ryan, 2010). Consistent with our model, calcineurin has been reported to regulate bulk synaptic vesicle endocytosis during periods of intense activity (Clayton et al., 2009). In addition, evidence for roles of calcineurin α and β catalytic isoforms in regulating synaptic vesicle endocytosis has been reported recently (Sun et al., 2010). Further examination of the mechanisms by which each calcineurin isoform regulates presynaptic function in cortical neurons is of considerable interest.

Our finding of reduced dynamin I expression in PFC of schizophrenia patients suggests that similar presynaptic mechanisms may contribute to cognitive deficits in schizophrenia. The observed hyperphosphorylation of presynaptic substrates in the CN-KO PFC and reduction in total dynamin I protein levels in schizophrenia PFC may represent a common mechanism if hyperphosphorylated dynamin I is more vulnerable to degradation pathways in the human PFC. Alternatively, dysfunction of different pathways in the CN-KO mouse and schizophrenia patients

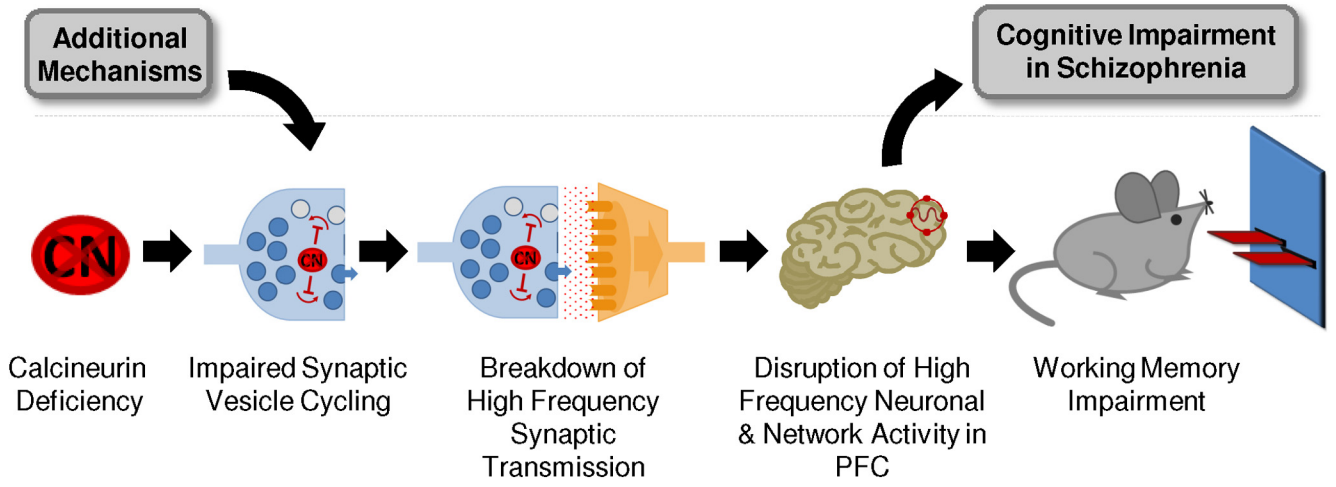

Figure 7. A presynaptic model for working memory deficits. Calcineurin deficiency impairs the ability of neurons in PFC to efficiently mobilize and recycle synaptic vesicles during high-frequency activity, leading to a disruption of high-frequency neuronal and network activities in PFC that are required for working memory. Additional molecular alterations implicated in schizophrenia may converge on the synaptic vesicle cycle and thereby contribute to specific cognitive impairments associated with the disease.

may converge on disruption of presynaptic function with distinct molecular manifestations. Consistent with this concept, mounting evidence from gene profiling, genetic association, and proteomic analyses indicates that alterations in presynaptic function contribute to the etiology of schizophrenia (Chen et al., 2004; Lee et al., 2005; Behan et al., 2009; Maycox et al., 2009; Faludi and Mirnics, 2011). In addition, several studies have reported alterations in presynaptic function or short-term synaptic plasticity in other mouse models of schizophrenia (Jentsch et al., 2009; Talbot, 2009; Blundell et al., 2010; Earls et al., 2010; Kvajo et al., 2011). Critically, our study extends on these findings by revealing an integrated disease mechanism that links presynaptic dysfunction with corresponding effects on higher-order circuit, network, and cognitive functions. Based on this collective body of work, we hypothesize that synaptic vesicle cycling represents a common node that can be disrupted by various genetic, developmental, or environmental insults leading to impaired cognitive function in schizophrenia. Future studies are required to elucidate the potential convergence of these various disease factors on the presynaptic vesicle cycling machinery.

A current schizophrenia disease hypothesis posits that impaired function of parvalbumin-positive interneurons (PV-IN) in the cortex is a key contributing factor in network dysfunction associated with cognitive deficits in schizophrenia (Gonzalez-Burgos et al., 2011). Activity of fast spiking PV-IN neurons is essential for generating high-frequency network activity in cortex, and loss of function in PV-IN ultimately results in a disruption of synchronous, cortical activity (Gonzalez-Burgos et al., 2011). In the CN-KO mice used in our study, calcineurin is removed selectively from glutamatergic neurons (Zeng et al., 2001), suggesting that specific deficits in the excitatory arm of the cortical network may result in impaired cortical synchrony and supporting the idea that disruptions of excitatory-inhibitory balance represent an underlying factor in network dysfunction in schizophrenia. Our results are thus consistent with the PV-IN impairment hypothesis and support the general concept that multiple mechanisms leading to reductions in synchrony in PFC could contribute to cognitive impairments associated with schizophrenia. Importantly, it is also possible that the number and/or function of cortical PV-INs are altered indirectly via the deletion of calcineurin from excitatory neurons in the cortex and hippocampus. It will be of considerable interest to examine the function of cortical inhibitory neurons in CN-KO mice.

In the present study, we demonstrated a disruption of γ oscillations in the PFC of CN-KO and CN-Het mice while they are exploring a novel environment and a disruption in performance of a nonspatial, operant working memory task (DNMTP). A similar correlation between disruption of γ oscillations and working memory impairment was observed in mice in which *N*-methyl-D-aspartate receptors were selectively disrupted in PV-INs (Carlen et al., 2012). These findings raise important questions regarding the role of oscillatory activity in working memory function in mice. Studies in humans have shown that the intensity of γ oscillations in the PFC during performance of a related delayed nonmatch to sample task correlates with performance in the task (Park et al., 2012; Roux et al., 2012). Based on these data, we would expect a decrease in γ oscillatory power in the CN-KO and CN-Het mice during performance of the DNMTP task. Future studies will address this question.

There is evidence that a disruption in synchrony between the hippocampus and the PFC contributes to working memory impairments in schizophrenia patients (Meyer-Lindenberg et al., 2005) as well as in mouse models of the disease (Sigurdsson et al., 2010). It is possible that, by impairing high-frequency network activity in either or both brain regions, altered synaptic vesicle cycling contributes directly to disruptions in hippocampal-PFC synchrony, although it is also possible that the two mechanisms are independent. In this regard, examination of PFC-hippocampal synchrony in CN-KO mice will be informative.

In conclusion, our analysis of cortical function in CN-KO mice provides support for a presynaptic mechanism for working memory dysfunction. Our results are aligned with a body of emerging evidence for presynaptic alterations in a number of CNS disorders (Waites and Garner, 2011). Interestingly, a recent report described a presynaptic mechanism of action for several antipsychotic compounds (Tischbirek et al., 2012). Collectively, these findings strongly support the concept that therapeutic approaches targeting presynaptic function are warranted. A synaptic functional screening technology enabling this therapeutic discovery strategy was recently described (Hempel et al., 2011). Moreover, phenotypic screening approaches have proven to be particularly effective in CNS drug discovery (Swinney and An-

thony, 2011). Hopefully, the insights gained from our study will ultimately contribute to the discovery of novel mechanism-based therapies for cognitive impairments in schizophrenia and other CNS disorders.

References

Baddeley A (2012) Working memory: theories, models, and controversies. Annu Rev Psychol 63:1–29. CrossRef Medline

Bartos M, Vida I, Jonas P (2007) Synaptic mechanisms of synchronized γ oscillations in inhibitory interneuron networks. Nat Rev Neurosci 8:45–56. CrossRef Medline

Behan AT, Byrne C, Dunn MJ, Cagney G, Cotter DR (2009) Proteomic analysis of membrane microdomain-associated proteins in the dorsolateral prefrontal cortex in schizophrenia and bipolar disorder reveals alterations in LAMP, STXBP1 and BASP1 protein expression. Mol Psychiatry 14:601–613. CrossRef Medline

Blundell J, Kaeser PS, Südhof TC, Powell CM (2010) RIM1α and interacting proteins involved in presynaptic plasticity mediate prepulse inhibition and additional behaviors linked to schizophrenia. J Neurosci 30:5326–5333. CrossRef Medline

Calabrese P (2006) Neuropsychology of multiple sclerosis: an overview. J Neurol 253 [Suppl 1]:I10–15.

Carlén M, Meletis K, Siegle JH, Cardin JA, Futai K, Vierling-Claassen D, Rühlmann C, Jones SR, Deisseroth K, Sheng M, Moore CI, Tsai LH (2012) A critical role for NMDA receptors in parvalbumin interneurons for γ rhythm induction and behavior. Mol Psychiatry 17:537–548. CrossRef Medline

Castaneda AE, Tuulio-Henriksson A, Marttunen M, Suvisaari J, Lönnqvist J (2008) A review on cognitive impairments in depressive and anxiety disorders with a focus on young adults. J Affect Disord 106:1–27. CrossRef Medline

Chen Q, He G, Wang XY, Chen QY, Liu XM, Gu ZZ, Liu J, Li KQ, Wang SJ, Zhu SM, Feng GY, He L (2004) Positive association between synapsin II and schizophrenia. Biol Psychiatry 56:177–181. CrossRef Medline

Clayton EL, Anggono V, Smillie KJ, Chau N, Robinson PJ, Cousin MA (2009) The phospho-dependent dynamin-syndapin interaction triggers activity-dependent bulk endocytosis of synaptic vesicles. J Neurosci 29:7706–7717. CrossRef Medline

Cousin MA, Robinson PJ (2001) The dephosphins: dephosphorylation by calcineurin triggers synaptic vesicle endocytosis. Trends Neurosci 24:659–665. CrossRef Medline

Cremona O, Di Paolo G, Wenk MR, Lüthi A, Kim WT, Takei K, Daniell L, Nemoto Y, Shears SB, Flavell RA, McCormick DA, De Camilli P (1999) Essential role of phosphoinositide metabolism in synaptic vesicle recycling. Cell 99:179–188. CrossRef Medline

Di Paolo G, Sankaranarayanan S, Wenk MR, Daniell L, Perucco E, Caldarone BJ, Flavell R, Picciotto MR, Ryan TA, Cremona O, De Camilli P (2002) Decreased synaptic vesicle recycling efficiency and cognitive deficits in amphiphysin 1 knock-out mice. Neuron 33:789–804. CrossRef Medline

Di Paolo G, Moskowitz HS, Gipson K, Wenk MR, Voronov S, Obayashi M, Flavell R, Fitzsimonds RM, Ryan TA, De Camilli P (2004) Impaired PtdIns(4,5)P2 synthesis in nerve terminals produces defects in synaptic vesicle trafficking. Nature 431:415–422. CrossRef Medline

Doyle AE (2006) Executive functions in attention-deficit/hyperactivity disorder. J Clin Psychiatry 67 [Suppl 8]:21–26.

Earls LR, Bayazitov IT, Fricke RG, Berry RB, Illingworth E, Mittleman G, Zakharenko SS (2010) Dysregulation of presynaptic calcium and synaptic plasticity in a mouse model of 22q11 deletion syndrome. J Neurosci 30:15843–15855. CrossRef Medline

Faludi G, Mirnics K (2011) Synaptic changes in the brain of subjects with schizophrenia. Int J Dev Neurosci 29:305–309. CrossRef Medline

Ferguson SM, De Camilli P (2012) Dynamin, a membrane-remodelling GTPase. Nat Rev Mol Cell Biol 13:75–88. CrossRef Medline

Ferguson SM, Brasnjo G, Hayashi M, Wölfel M, Collesi C, Giovedi S, Raimondi A, Gong LW, Ariel P, Paradise S, O'Toole E, Flavell R, Cremona O, Miesenböck G, Ryan TA, De Camilli P (2007) A selective activity-dependent requirement for dynamin 1 in synaptic vesicle endocytosis. Science 316:570–574. CrossRef Medline

Funahashi S, Bruce CJ, Goldman-Rakic PS (1989) Mnemonic coding of visual space in the monkey's dorsolateral prefrontal cortex. J Neurophysiol 61:331–349. Medline

Funahashi S, Chafee MV, Goldman-Rakic PS (1993) Prefrontal neuronal activity in rhesus monkeys performing a delayed anti-saccade task. Nature 365:753–756. CrossRef Medline

Gerber DJ, Hall D, Miyakawa T, Demars S, Gogos JA, Karayiorgou M, Tonegawa S (2003) Evidence for association of schizophrenia with genetic variation in the 8p21.3 gene, PPP3CC, encoding the calcineurin γ subunit. Proc Natl Acad Sci U S A 100:8993–8998. CrossRef Medline

Goldman-Rakic PS (1990) Cellular and circuit basis of working memory in prefrontal cortex of nonhuman primates. Prog Brain Res 85:325–335; discussion 335–326. Medline

Goldman-Rakic PS (1995) Cellular basis of working memory. Neuron 14:477–485. CrossRef Medline

Gonzalez-Burgos G, Fish KN, Lewis DA (2011) GABA neuron alterations, cortical circuit dysfunction and cognitive deficits in schizophrenia. Neural Plast 2011:723184. CrossRef Medline

Gonzalez-Sulser A, Wang J, Motamedi GK, Avoli M, Vicini S, Dzakpasu R (2011) The 4-aminopyridine in vitro epilepsy model analyzed with a perforated multi-electrode array. Neuropharmacology 60:1142–1153. CrossRef Medline

Granseth B, Odermatt B, Royle SJ, Lagnado L (2006) Clathrin-mediated endocytosis is the dominant mechanism of vesicle retrieval at hippocampal synapses. Neuron 51:773–786. CrossRef Medline

Groth RD, Dunbar RL, Mermelstein PG (2003) Calcineurin regulation of neuronal plasticity. Biochem Biophys Res Commun 311:1159–1171. CrossRef Medline

Hempel CM, Sivula M, Levenson JM, Rose DM, Li B, Sirianni AC, Xia E, Ryan TA, Gerber DJ, Cottrell JR (2011) A system for performing high throughput assays of synaptic function. PLoS One 6:e25999. CrossRef Medline

Horiuchi Y, Ishiguro H, Koga M, Inada T, Iwata N, Ozaki N, Ujike H, Muratake T, Someya T, Arinami T (2007) Support for association of the PPP3CC gene with schizophrenia. Mol Psychiatry 12:891–893. CrossRef Medline

Huntley J, Bor D, Hampshire A, Owen A, Howard R (2011) Working memory task performance and chunking in early Alzheimer's disease. Br J Psychiatry 198:398–403. CrossRef Medline

Irizarry RA, Bolstad BM, Collin F, Cope LM, Hobbs B, Speed TP (2003) Summaries of Affymetrix GeneChip probe level data. Nucleic Acids Res 31:e15. CrossRef Medline

Jentsch JD, Trantham-Davidson H, Jairl C, Tinsley M, Cannon TD, Lavin A (2009) Dysbindin modulates prefrontal cortical glutamatergic circuits and working memory function in mice. Neuropsychopharmacology 34:2601–2608. CrossRef Medline

Jovanovic JN, Sihra TS, Nairn AC, Hemmings HC Jr, Greengard P, Czernik AJ (2001) Opposing changes in phosphorylation of specific sites in synapsin I during Ca^{2+}-dependent glutamate release in isolated nerve terminals. J Neurosci 21:7944–7953. Medline

Kavalali ET (2006) Synaptic vesicle reuse and its implications. Neuroscientist 12:57–66. CrossRef Medline

Kim SH, Ryan TA (2010) CDK5 serves as a major control point in neurotransmitter release. Neuron 67:797–809. CrossRef Medline

Kurtz MM, Wexler BE, Fujimoto M, Shagan DS, Seltzer JC (2008) Symptoms versus neurocognition as predictors of change in life skills in schizophrenia after outpatient rehabilitation. Schizophr Res 102:303–311. CrossRef Medline

Kvajo M, McKellar H, Drew LJ, Lepagnol-Bestel AM, Xiao L, Levy RJ, Blazeski R, Arguello PA, Lacefield CO, Mason CA, Simonneau M, O'Donnell JM, MacDermott AB, Karayiorgou M, Gogos JA (2011) Altered axonal targeting and short-term plasticity in the hippocampus of Disc1 mutant mice. Proc Natl Acad Sci U S A 108:E1349–E1358. CrossRef Medline

Lee HJ, Song JY, Kim JW, Jin SY, Hong MS, Park JK, Chung JH, Shibata H, Fukumaki Y (2005) Association study of polymorphisms in synaptic vesicle-associated genes, SYN2 and CPLX2, with schizophrenia. Behav Brain Funct 1:15. CrossRef Medline

Leussis MP, Bolivar VJ (2006) Habituation in rodents: a review of behavior, neurobiology, and genetics. Neurosci Biobehav Rev 30:1045–1064. CrossRef Medline

Liu YL, Fann CS, Liu CM, Chang CC, Yang WC, Hung SI, Yu SL, Hwang TJ, Hsieh MH, Liu CC, Tsuang MM, Wu JY, Jou YS, Faraone SV, Tsuang MT, Chen WJ, Hwu HG (2007) More evidence supports the association of PPP3CC with schizophrenia. Mol Psychiatry 12:966–974. CrossRef Medline

Maycox PR, Kelly F, Taylor A, Bates S, Reid J, Logendra R, Barnes MR,

Larminie C, Jones N, Lennon M, Davies C, Hagan JJ, Scorer CA, Angelinetta C, Akbar MT, Hirsch S, Mortimer AM, Barnes TR, de Belleroche J (2009) Analysis of gene expression in two large schizophrenia cohorts identifies multiple changes associated with nerve terminal function. Mol Psychiatry 14:1083–1094. CrossRef Medline

Mesholam-Gately RI, Giuliano AJ, Goff KP, Faraone SV, Seidman LJ (2009) Neurocognition in first-episode schizophrenia: a meta-analytic review. Neuropsychology 23:315–336. CrossRef Medline

Meyer-Lindenberg AS, Olsen RK, Kohn PD, Brown T, Egan MF, Weinberger DR, Berman KF (2005) Regionally specific disturbance of dorsolateral prefrontal-hippocampal functional connectivity in schizophrenia. Arch Gen Psychiatry 62:379–386. CrossRef Medline

Miyakawa T, Leiter LM, Gerber DJ, Gainetdinov RR, Sotnikova TD, Zeng H, Caron MG, Tonegawa S (2003) Conditional calcineurin knockout mice exhibit multiple abnormal behaviors related to schizophrenia. Proc Natl Acad Sci U S A 100:8987–8992. CrossRef Medline

Monoranu CM, Apfelbacher M, Grünblatt E, Puppe B, Alafuzoff I, Ferrer I, Al-Saraj S, Keyvani K, Schmitt A, Falkai P, Schittenhelm J, Halliday G, Kril J, Harper C, McLean C, Riederer P, Roggendorf W (2009) pH measurement as quality control on human post mortem brain tissue: a study of the BrainNet Europe consortium. Neuropathol Appl Neurobiol 35:329–337. CrossRef Medline

Park JY, Lee KS, An SK, Lee J, Kim JJ, Kim KH, Namkoong K (2012) Gamma oscillatory activity in relation to memory ability in older adults. Int J Psychophysiol 86:58–65. CrossRef Medline

Roux F, Wibral M, Mohr HM, Singer W, Uhlhaas PJ (2012) Gamma-band activity in human prefrontal cortex codes for the number of relevant items maintained in working memory. J Neurosci 32:12411–12420. CrossRef Medline

Rusnak F, Mertz P (2000) Calcineurin: form and function. Physiol Rev 80:1483–1521. Medline

Ryan TA (1999) Inhibitors of myosin light chain kinase block synaptic vesicle pool mobilization during action potential firing. J Neurosci 19:1317–1323. Medline

Sigurdsson T, Stark KL, Karayiorgou M, Gogos JA, Gordon JA (2010) Impaired hippocampal-prefrontal synchrony in a genetic mouse model of schizophrenia. Nature 464:763–767. CrossRef Medline

Sun T, Wu XS, Xu J, McNeil BD, Pang ZP, Yang W, Bai L, Qadri S, Molkentin JD, Yue DT, Wu LG (2010) The role of calcium/calmodulin-activated calcineurin in rapid and slow endocytosis at central synapses. J Neurosci 30:11838–11847. CrossRef Medline

Swinney DC, Anthony J (2011) How were new medicines discovered? Nat Rev Drug Discov 10:507–519. CrossRef Medline

Talbot K (2009) The sandy (sdy) mouse: a dysbindin-1 mutant relevant to schizophrenia research. Prog Brain Res 179:87–94. CrossRef Medline

Tischbirek CH, Wenzel EM, Zheng F, Huth T, Amato D, Trapp S, Denker A, Welzel O, Lueke K, Svetlitchny A, Rauh M, Deusser J, Schwab A, Rizzoli SO, Henkel AW, Müller CP, Alzheimer C, Kornhuber J, Groemer TW (2012) Use-dependent inhibition of synaptic transmission by the secretion of intravesicularly accumulated antipsychotic drugs. Neuron 74:830–844. CrossRef Medline

Uhlhaas PJ, Singer W (2010) Abnormal neural oscillations and synchrony in schizophrenia. Nat Rev Neurosci 11:100–113. CrossRef Medline

Uhlhaas PJ, Haenschel C, Nikoliæ D, Singer W (2008) The role of oscillations and synchrony in cortical networks and their putative relevance for the pathophysiology of schizophrenia. Schizophr Bull 34:927–943. CrossRef Medline

Waites CL, Garner CC (2011) Presynaptic function in health and disease. Trends Neurosci 34:326–337. CrossRef Medline

Weinberger DR, Aloia MS, Goldberg TE, Berman KF (1994) The frontal lobes and schizophrenia. J Neuropsychiatry Clin Neurosci 6:419–427. Medline

Wiig KA, Burwell RD (1998) Memory impairment on a delayed nonmatching-to-position task after lesions of the perirhinal cortex in the rat. Behav Neurosci 112:827–838. CrossRef Medline

Wiig KA, Whitlock JR, Epstein MH, Carpenter RL, Bear MF (2009) The levo enantiomer of amphetamine increases memory consolidation and gene expression in the hippocampus without producing locomotor stimulation. Neurobiol Learn Mem 92:106–113. CrossRef Medline

Zeng H, Chattarji S, Barbarosie M, Rondi-Reig L, Philpot BD, Miyakawa T, Bear MF, Tonegawa S (2001) Forebrain-specific calcineurin knockout selectively impairs bidirectional synaptic plasticity and working/episodic-like memory. Cell 107:617–629. CrossRef Medline